Aerospace Science and Technology 54 (2016) 143–150

Contents lists available at ScienceDirect

Aerospace Science and Technology

www.elsevier.com/locate/aescte

Design of predictive control and evaluate the effects of flight dynamics on performance of one axis gimbal system, considering disturbance torques

A.R. Toloei [a], M. Pirzadeh [b,*], A.R. Vali [c]

[a] Department of Aerospace, Shahid Beheshti University, Tehran, Iran
[b] Department of Electrical Engineering, Damavand Branch, Islamic Azad University, Damavand, Iran
[c] Department of Electrical Engineering, Malek-Ashtar University of Technology (MUT), Tehran, Iran

ARTICLE INFO

Article history:
Received 28 September 2015
Received in revised form 16 April 2016
Accepted 19 April 2016
Available online 20 April 2016

Keywords:
Disturbance torques
Flight dynamics
Gimbal friction
Line of sight MPC
Stabilization loop

ABSTRACT

In this paper, we aim to present control of one axis gimbal system. Indeed, the purpose of using the model of predictive control is twofold. Firstly, it runs the stabilization loop. Stabilization loop is constructed with DC motor, Rate Gyro and inertia utilizing MPC type controller. The gimbal torque relationships are obtained from using Newton's second law equation on the assumption that gimbal is rigid body. The second purpose is to analyze the effects of flight dynamics on performance of one axis gimbal system. A set of scenarios' tests is performed to evaluate the act of the proposed system in various conditions, considering the gimbal friction, mass imbalance and disturbance torques. SIMULINK/MATLAB is administered to assess the entire control system. The simulation results are discussed to show the validity of the proposed system during the flight and show that the gimbal system stabilizes the line of sight even when the disturbance torques affect the system performance.

1. Introduction

Generally, guided missiles which are aerodynamically unstable in all or part of the flight path need control system for stability. Missile test flights are very expensive. Moreover, they are not reusable after a test launch. Although, the seeker system was tested independently for both stabilization and tracking loop under trajectory dynamic conditions without the guidance loop, there is no sufficient insight for upgrading seeker design, while it helped to validate the simulator software. 6-DOF model with seeker and other subsystems has been validated a priority. The simulations are based on mathematical models of missiles, targets and environmental conditions, which can provide valuable information about the performance of the missile subsystem [1,2]. In [1], the model of one axis gimbal system is introduced with PI controller and analyzes the effects of flight dynamics on performance of one axis gimbal system. Today, control design methods based on the MPC concept have found a wide usage in many important industrial applications and have been studied by academia. Reasons for such popularities include the ability and industrial approach. MPC is based on an optimization method that uses a system model to predict the effect of a control action applied on the system [3]. In [4], the benefits of MPC within an electro-optic (EO) system track loop is introduced by using the MPC guidance controller and the simple model. Though the effects of torque disturbances and Flight Dynamics on Performance of system are not considered. An indirect adaptive predictive idea for controlling the pitch channel autopilot from Vanguard missile is proposed in [5]. In [6], new approaches properly calibrate the laser tracking system (LTS) prior to using it for metrology and improving the measured accuracy of LTS. In [6,21], a kinematic model for the single-beam tracker is suggested in which a necessary and an adequate number of kinematic parameters are used. The model of mass imbalance is created by analyzing the relationships among the mass imbalance, the friction, the current of motor, and the attitude of gimbal. However, it rejects the disturbances, with the use of the cascade PID controller to control the system. Gimbal torque relationships are derived by taking into consideration the base angular motion. The performance of model with constant LOS rate values and disturbances were also investigated in [7]. [8] explored four methods of Model-based controllers (proportional–integral (PI), internal model control (IMC), sliding mode control (SMC), and model predictive sliding mode control (MPSMC) for reducing the hysteretic effect of THUNDER actuator. In [9], a constrained MPC for helicopter models was used which are obtained by physical considerations. Also, it showed significant promise for robust tracking. Furthermore, by

* Corresponding author.
E-mail address: meisam.pirzadeh67@gmail.com (M. Pirzadeh).

http://dx.doi.org/10.1016/j.ast.2016.04.019
1270-9638/

using the MPC method, [10] investigated the feasibility of controlling a small-scale autonomous unmanned helicopter. In [11], a method for disturbance rejection in the stabilization loop was provided by using the multilayer neural-net-based feedforward controller. The researchers provided the fuzzy PID type controller for one axis gimbal system and evaluated the performance of system for both conventional PI and fuzzy PID controller, in [12,17]. Also, the models were tested for constant and hypothetical body angular motions. A robust control for disturbance rejection in yaw – pitch gimballed system to actuator saturation and disturbances was also designed. Analysis was done for different disturbances, including state couplings, platform angular motion and disturbance torque inputs. Yet, the effect of flight dynamics was not considered in [13]. In [14], a practical three-mass model for the direct-drive gimballed platform from the motor to the antenna was introduced. Moreover, PI^2L controller was used to stabilize in the stabilization loop. In [15], to analyze friction as well as mass imbalance, a model-based method was used which mainly affected the accuracy of ISP. The model of mass imbalance was created through analyzing the relationships between the mass imbalance, the friction, the current of motor, and the attitude of gimbal. Also, in order to reject the disturbances, the model based feedforward compensation system was added to the PID control system. In [16], fuzzy PID type controller was used for a two axis gimbal system and evaluated the performance of the system for both conventional PI and fuzzy PID controller. The models tested for constant LOS rate values and disturbances as well. A method was offered by [18] for measuring and correcting static imbalances and the principles of reducing dynamic imbalance in gimbals in order to reduce disturbance response. In [19], the finite-horizon tracking technique was used based on change of variables that converted the differential Riccati equation to a linear Lyapunov equation. Via numerical implementation, the structure of the 6-DOF model was evaluated regarding the measure of desired seeker angles. In [20], to reduce the platform disturbance that couples with the gimbal inner axis (elevation axis), angular rate of the seeker was used considering the 2-DOF internal model controller. The performance of model with constant LOS rate values and disturbances was also investigated. [22] provided the model of two degrees of freedom (2-DOF) gimbal system and its torque relationships obtained from a simplified model supposing that each gimbal is balanced.

In this research, for estimating the total uncertainty, the researcher evaluates the performance of gimbal system that tests one axis gimbal system taking into account flight dynamics and 6-DOF equations of motion. To do so, first of all, the stabilization system is constructed so that the several disturbance torques are included. Then, the MPC controller is used to control the stabilization loop. Then, the airframe is constructed which includes the forces, moments, aerodynamic coefficients, environment models, and equations of motion. Afterwards, guidance unit, autopilot and target specifications are modeled. Also, the system is modeled based on using SIMULINK/MATLAB. At the end, one axis gimbal system with missile dynamics, guidance and control loops, is tested for disturbance torques and angular velocities which are imposed online from missile frame to seeker. In the rest of the paper, the gimbal system is presented and compared under the terms of offline and online.

2. Problem formulation

Evaluating the performance of the stabilization loop control, and testing the flight path are very momentous. So, it is important to achieve the relationships among forces, moments and kinematic equations. External forces and moments are produced by aerodynamic coefficients.

2.1. Missile equations of motion

Analysis of the flight of a flying object is dependent on the equations of motion. These equations are a starting point in finding the dynamic characteristics of the flying object. The airframe dynamics are calculated on the basis of using of the motion's equations for a rigid body. The translational motion of a body is defined as the acceleration of the body's center of mass that is measured from an inertial reference. If the moving frame is connected to the center of mass of the body, the scalar equations are as follows [1, 23]:

$$\begin{aligned}
&(X + \text{Thrust}) + g_X = m(\dot{u} + qw - rv)\\
&Y + g_Y = m(\dot{v} + ru - pw)\\
&Z + g_Z = m(\dot{w} - qu + pv)
\end{aligned} \tag{1}$$

(g_X, g_Y, g_Z) are components of gravitational force vector expresses in the body coordinate system. The components of the angular momentum are calculated on the axes of a frame connected to the center of mass and moved with the body. Therefore, rotational equations are equal to [1,23]:

$$\begin{aligned}
&\dot{p} = M_X/I_X + qr(I_Y - I_Z)/I_X\\
&\dot{q} = M_Y/I_Y + rp(I_Z - I_X)/I_Y\\
&\dot{r} = M_Z/I_Z + pq(I_X - I_Y)/I_Z
\end{aligned} \tag{2}$$

(p, q, r) are the components of the angular velocity vector about the body (x, y, z) axes. A numerical expression of the situation of an object relative to a coordinate system is very important. One of the best methods for expression of attitude, is the Euler angle method. Therefore, equation (3) is the Euler angles [1,23]:

$$\begin{aligned}
&\dot{\theta} = q\cos\varphi - r\sin\varphi\\
&\dot{\varphi} = p + \dot{\psi}\sin\theta\\
&\dot{\psi} = (r\cos\varphi + q\sin\varphi)/\cos\theta
\end{aligned} \tag{3}$$

Generally, (φ, θ, ψ) are Euler angles.

2.2. AirFrame

An equation of motion exists for each degree of freedom. The airframe can have any configuration, so this is expressed in the aerodynamic data that is used to compute the aerodynamic forces and moments, moments of inertia and products of inertia in the equations of rotational motion. These are given by [1,23]:

$$\begin{aligned}
&F_X = q_0 S_{ref} C_X\\
&F_Y = q_0 S_{ref} C_Y\\
&F_Z = q_0 S_{ref} C_Z
\end{aligned} \tag{4}$$

Here, $q_0 = 0.5\rho V^2$ is a free stream dynamic pressure and S_{ref} is a reference area. Further, ρ is the density of the atmosphere and V is the magnitude of the wind-corrected velocity or airspeed. The whole of aerodynamic moment is calculated on the body coordinate system and is determined by [1,23]:

$$\begin{aligned}
&M_X = C_l q_0 S_{ref} I_{refy}\\
&M_Y = C_m q_0 S_{ref} I_{refx}\\
&M_Z = C_n q_0 S_{ref} I_{refy}
\end{aligned} \tag{5}$$

In equation (5), I_{ref} is the reference length of body.

The force coefficients (C_X, C_Y, C_Z) computed for the various aerodynamic affects acting on the airframe. The coefficients are

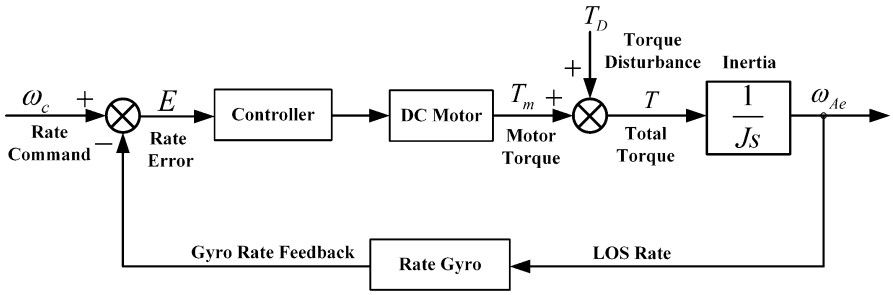

Fig. 1. One axis inertial stabilized platform [1,7].

referenced to the body axes and are non-dimensional. The functional form for the linearized aerodynamic force coefficients in the body coordinate system is given by [1,23]:

$$C_X = C_{X_0}$$
$$C_Y = C_{Y_\beta}\beta + C_{Y_{\delta_r}}\delta_r + C_{Y_r} r(I_{refy}/2V)$$
$$C_Z = C_{Z_\alpha}\alpha + C_{Y_{\delta_e}}\delta_e + C_{Z_q} q(I_{refx}/2V) \tag{6}$$

Where α and β are the angle of attack and sideslip angle, respectively. Also, it is assumed that, Flying object is symmetric, $C_{Z_\alpha} = C_{Y_\beta}$, $C_{Z_q} = C_{Y_r}$ and $I_{refx} = I_{refy}$. The aerodynamic moment coefficients can be linearized just as the aerodynamic force coefficients are to yield [1,23]:

$$C_l = C_{l_{\delta_a}}\delta_a + C_{l_p} p(I_{refy}/2V) + C_{l_\beta}\beta$$
$$C_m = C_{m_\alpha}\alpha + C_{m_{\delta_e}}\delta_e + C_{m_q} q(I_{refx}/2V)$$
$$C_n = C_{n_\beta}\beta + C_{n_{\delta_r}}\delta_r + C_{n_r} r(I_{refx}/2V) \tag{7}$$

In equation (7), $(\delta_a, \delta_e, \delta_r)$ are angle of effective control-surface deflection.

3. One axis gimbal system

The gimbal stabilization mechanism system is used to provide the stability with an object mounted on the gimbal by isolating it from the base angular motion and vibration [1]. The stabilization loop system is shown in Fig. 1, which represents the block diagram of the gimbal control system. Also, its configuration is generic for a stabilization loop. The control system is an attempt to null the difference between the rate command input and the angular rate of the gimbal.

Newton's second law in this case is:

If a net torque T is applied to a homogeneous rigid mass, it will have a moment of inertia J, afterward, the body will develop an angular acceleration α [1,7] according to:

$$T = J.\alpha \tag{8}$$

So, all what is needed is to stop the rotation of an object with respect to inertial space. It is ensured that the applied torque is zero. Nevertheless, the effects of torque disturbances should not be ignored; since, this ignorance will lead to excessive movement and vibration LOS. Besides, the rotation of a means for controlling the object is needed in response to command inputs, which is called rate gyro. Rate gyro typically connects the object to measuring the inertia rotation about the axes which need stabilization and control. The gyro is used in a closed-loop servo system to nullify the disturbances and, at the same time, allow the object to be controlled from external command inputs [1,7]. The one axis stabilized gimbal is shown in Fig. 2.

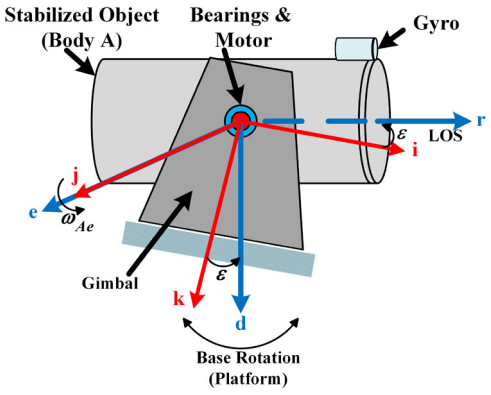

Fig. 2. One axis stabilized gimbal [1,7].

3.1. Mathematical model of gimbal motion

The stabilized object is placed on the gimbal, and gimbal is regarded as rigid body. Two reference frames are identified. Frame P fixes the fuselage body (platform) with axes (i, j, k), and frame A fixes the gimbal with axes (r, e, d). The body-fixed frame P acts in conformity with the gimbal frame A by a positive angle of rotation ε (gimbal angle) on the e-axis. The r-axis coincides with the LOS axis. The k-axis is pointing "downwards". The center of rotation is at the frame origin, which is assumed to be the same point for the two frames. So, frame P concurs with frame A for $\varepsilon = 0$. Associated with this rotation, we have the following transformation [1,7]:

$$\overset{A}{P}C = \begin{bmatrix} \cos\varepsilon & 0 & -\sin\varepsilon \\ 0 & 1 & 0 \\ \sin\varepsilon & 0 & \cos\varepsilon \end{bmatrix} \tag{9}$$

Where $\overset{A}{P}C$ is the transformation from frame P to frame A. The inertial angular velocity vectors of frames P and A, is respectively given by [1,7]:

$${}^{p}\vec{\omega}_{P/I} = \begin{bmatrix} \omega_{pi} \\ \omega_{pj} \\ \omega_{pk} \end{bmatrix}, \qquad {}^{A}\vec{\omega}_{A/I} = \begin{bmatrix} \omega_{Ar} \\ \omega_{Ae} \\ \omega_{Ad} \end{bmatrix} \tag{10}$$

Where $(\omega_{p_i}, \omega_{p_j}, \omega_{p_k})$ are the body angular velocities of frame P in relation to inertial space about (i, j, k) axes respectively, and $(\omega_{A_r}, \omega_{A_e}, \omega_{A_d})$ are the gimbal angular velocities in relation to inertial space about the (r, e, d) axes respectively [1,7]. The angular velocities ω_{A_e} is the output of the control system for stabilization, and its aim is to make it possible to keep $\omega_{A_e} = 0$ despite disturbances. In addition, it keeps the nonrotating sensor in inertial space [7]. By using the transformation (9), the angular velocities of the stabilized are [1,7]:

$$\omega_{Ar} = \omega_{Pi}\cos\varepsilon - \omega_{Pk}\sin\varepsilon \tag{11a}$$

$$\omega_{Ae} = \omega_{Pj} + \dot{\varepsilon} \tag{11b}$$

$$\omega_{Ad} = \omega_{Pi} \sin\varepsilon + \omega_{Pk} \cos\varepsilon \tag{11c}$$

So, sum of the motor torque and external imperfection disturbance torques are given by using the above equations:

$$T_m = \dot{H}_e + \omega_{Ad} H_r - \omega_{Ar} H_d \tag{12}$$

Thus, they can be regarded as torque disturbances T_D, Fig. 1. When the platform is nonrotating ($\omega_{P_i} = \omega_{P_j} = \omega_{P_k} = 0$), the disturbance term is zero and just the motor torque T_m affects the body A.

4. Stabilization loop configuration

The stabilization loop is constructed with Rate Gyro, Platform, DC motor and Inertia utilizing MPC type controller.

Rate Gyro is used in this article as a second order system normally. It is assumed that the gyroscope dynamics is equal to [7];

ω_n (Natural Frequency) = 50 Hz,

ζ (Damping Ratio) = 0.7.

Therefor, the transfer function of gyro is:

$$G_{Gyro}(s) = \frac{2500}{(s^2 + 70s + 2500)} \tag{13}$$

The motor load is represented by the plateform which is connected to the shaft motor. The platform is modeled based on its moment of inertia that depends on its dimensions and position with respect to the axis of rotation. So, the moment of inertia is [7]:

$$J = \frac{1}{2} M r^2 = 9.8 \times 10^{-3}\ \mathrm{kg\,m^2} \tag{14}$$

It is considered that the platform specifications is M (Mass) = 1 kg, and r (Radius) = 14 cm, [7]. So, the transfer function of the DC motor is equal [1,7]:

$$G_m(s) = \frac{24637.68}{s^2 + 1500s + 20942}. \tag{15}$$

4.1. Proposed controller design

The Generalized Predictive Controller (GPC) is one of the most popular Model Predictive Controller methods. One of the aspects of MPC controller is the ability to perform on-line process optimization and use other control methods from the feedback. The past error is calculated, and finally, it makes current error. GPC methods are easy to use and they can be employed in self-tuning or even adaptive applications, Variable dead-time, and unstable/reverse-unstable plant which can be stably controlled by correct choices of horizon. A control horizon is utilized to reduce calculations. It does not need to start at 1 but it can range the possibility of adding control weighting [24] over the significant dynamical response. Thus, in this research, one axis gimbal system is stabilized to use the Generalized Predictive Control. Fig. 3 is selected as a proper block diagram to find out the GPC.

In Fig. 3 $d(t)$, $v(t)$ and $n(t)$ denote the output disturbance, the input disturbance and sensor noise correspondingly [5]. Also, parameters of controller are $R(z^{-1})$ and $S(z^{-1})$. This model is known as a CARIMA model (Controlled Auto Regressive and Integrated Moving Aver-age) and is given by:

$$A(z^{-1})y(t) = B(z^{-1})u_c(t-1) + T(z^{-1})e(t)/1 - z^{-1} \tag{16}$$

where, $e(t)$ is zero means white noise. (A, B, C) are the polynomial in the backward shift operator z^{-1}:

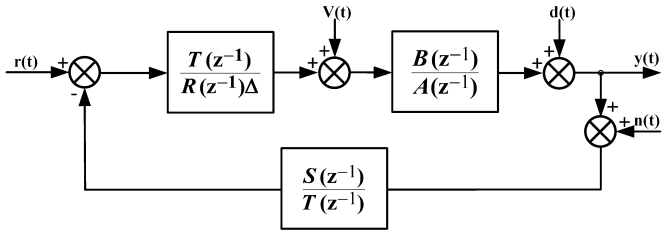

Fig. 3. GPC block diagram [5].

$$A(z^{-1}) = 1 + a_1 z^{-1} + a_2 z^{-2} + \cdots + a_{na} z^{-na}$$
$$B(z^{-1}) = b_0 + b_1 z^{-1} + b_2 z^{-2} + \cdots + b_{nb} z^{-nb}$$
$$T(z^{-1}) = 1 + t_1 z^{-1} + t_2 z^{-2} + \cdots + t_{nt} z^{-nt} \tag{17}$$

The main plan of GPC is to compute a sequence of future control signals. So, it minimizes the following multistage cost function that was defined over a prediction horizon [5]:

$$J(N_1, N_2, N_u) = \sum_{j=N_1}^{N_2} \delta(j)\big[\hat{y}(t+j|t) - w(t+j)\big]^2 + \sum_{j=1}^{N_u} \lambda(j)\big[\Delta u(t+j-1)\big]^2 \tag{18}$$

According to Eq. (18), $\hat{y}(t+j|t)$ is an optimum j-step ahead prediction of the system output from maximum prediction horizon to t. N_1 and N_2 are the minimum and maximum output horizons. N_u is the control horizon, and $\delta(j)$ and $\lambda(j)$ are weighting sequences. Furthermore, $r(t)$ or $w(t+j)$ represents the future reference trajectory [5]. According to [5], the control signal $u_c(t)$ is equal to:

$$\Delta u(t) = \frac{T(z^{-1})}{R(z^{-1})} r(t) - \frac{S(z^{-1})}{R(z^{-1})} y(t)$$
$$u_c(t) = \Delta u(t) + u_c(t-1) \tag{19}$$

Also, the output S_{yd} and noise-output S_{yn} sensitivity functions are determined:

$$S_{yd}(z^{-1}) = \frac{A(z^{-1})R(z^{-1})\Delta}{A(z^{-1})R(z^{-1})\Delta + B(z^{-1})S(z^{-1})z^{-1}}$$
$$S_{yn}(z^{-1}) = \frac{B(z^{-1})S(z^{-1})z^{-1}}{A(z^{-1})R(z^{-1})\Delta + B(z^{-1})S(z^{-1})z^{-1}} \tag{20}$$

By considering Fig. 4, GPC controller is added to stabilization loop in order to create the gain constant one and to keep steady state error zero. Fig. 4 shows how the closed loop control system produces a control torque at the motor that is equal and opposite of the pure disturbance torque. Thus, the rotating of object stops with respect to the inertial space.

5. Guidance and autopilot units

The guidance unit model implements to the simplest form of the PN navigation law. At first the PN guidance command components are computed in the detector frame from the estimates of the LOS rate components in antenna axes and the measured closing velocity (V_c). Then, components are calculated in the autopilot frame when transformed to the detector frame equal the required PN guidance components. The PN guidance commands in detector axes are [23]. These are limited to $\pm L = 20$ gees.

$$G_{Y_D} = N' \dot{R} r_{LD}/g$$
$$G_{Z_D} = -N' \dot{R} q_{LD}/g \tag{21}$$

Also, autopilot unit considers the dynamics of the first order. So, Fig. 5 shows the baseline model for flying object:

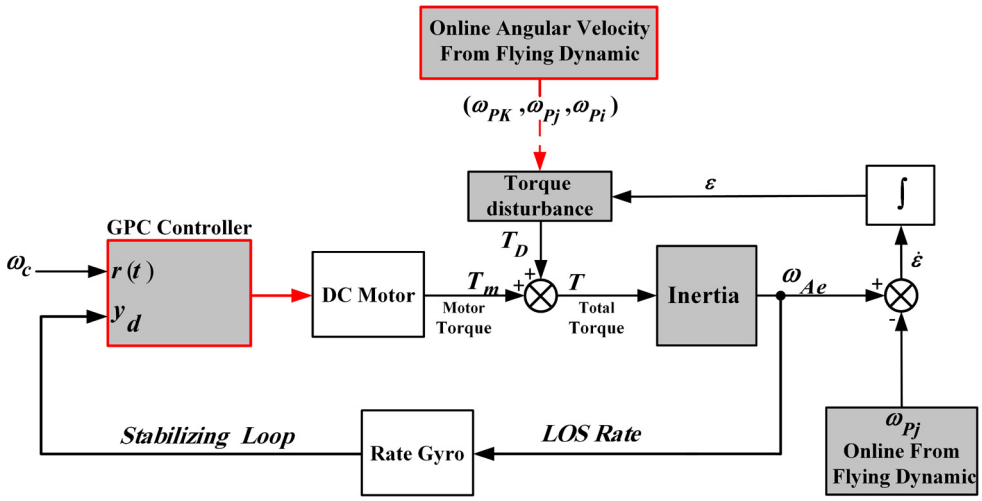

Fig. 4. One axis gimbal system with GPC controller.

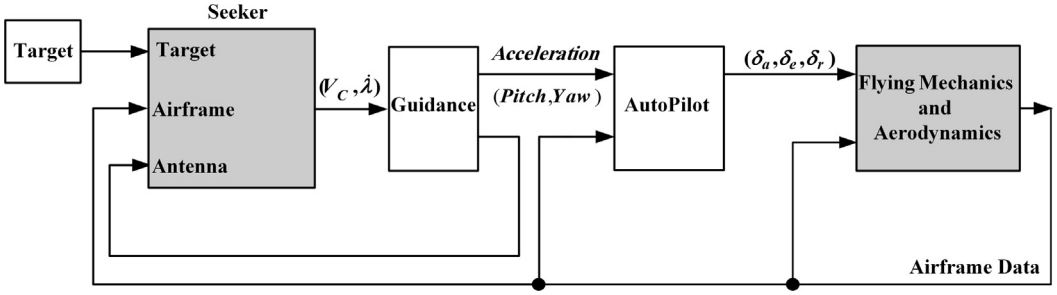

Fig. 5. Block diagram of baseline model [1].

Table 1
Physical parameters [1].

Parameter	Value
Length	5.08 m
Diameter	37 cm
Weight	584 kg
Speed	2.5 Mach

Table 2
Initial conditions [1].

Parameter	Initial value
Angle of attack α	0°
Position (x, y, z)	$(0, 0, -3.04)$ m
Angular rates (p, q, r)	$(0, 0, 0)$ deg/s
Euler angles (φ, θ, ψ)	$(0, \pi/4, 0)$
Missile velocity (V)	50 m/s
Mass	625 kg
Target velocity (V_t)	450 m/s

6. Simulations and results

The obtained model is tested for flight path, rate command input of online and platform angular rates. Firstly, it is imagined that the gimbal has no mass unbalance. Secondly, it is assumed that the gimbal contains mass unbalance. All stimulations are used SIMULINK and the difference between them is displayed on the same diagram to show the validity of the introduced model. Of course, the response of the MPC is compared to that of the traditional PI controller. Also, the physical parameters of the hypothetical missile is shown in Table 1.

The initial conditions for the missile launch are summarized in Table 2.

Also, Table 3 shows the test scenarios which consist of two parts:

A. Test condition is offline and the input rate command is 120°/s.
B. In this case, input rate and the body angular rate is derived from the airframe data and test condition is online.

When gimbal doesn't contain mass unbalance, the gimbal inertia matrix is diagonal and the disturbance torque is given in the following form [1,7]:

$$T_D = (A_d - A_r)\omega_{Ar}\omega_{Ad} \tag{22}$$

Here, gimbal contains mass unbalance. In these circumstances the gimbal inertia matrix is not diagonal and the disturbance torque is [1,7]:

Table 3
Test scenarios.

Scenarios	Test number	Angular rates (°/s)	Input rate (°/s)	Condition
A	1	$\omega_{Pj} = 0.61$, $\omega_{Pi} = 0$, $\omega_{Pk} = 0.25$	120°/s	Offline, without disturbance torques
	2	$\omega_{Pj} = 0.61$, $\omega_{Pi} = 0$, $\omega_{Pk} = 0.25$	120°/s	Offline, with disturbance torques
B	3	From airframe data	Online	Online, without disturbance torques
	4	From airframe data	Online	Online, with disturbance torques

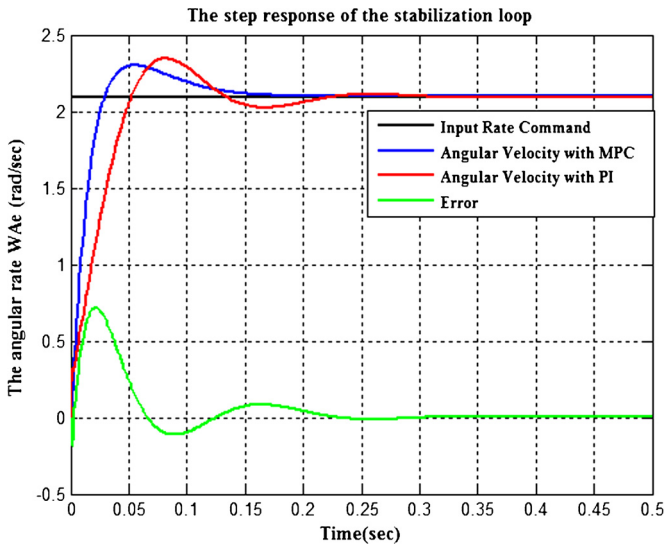

Fig. 6. Test number 1.

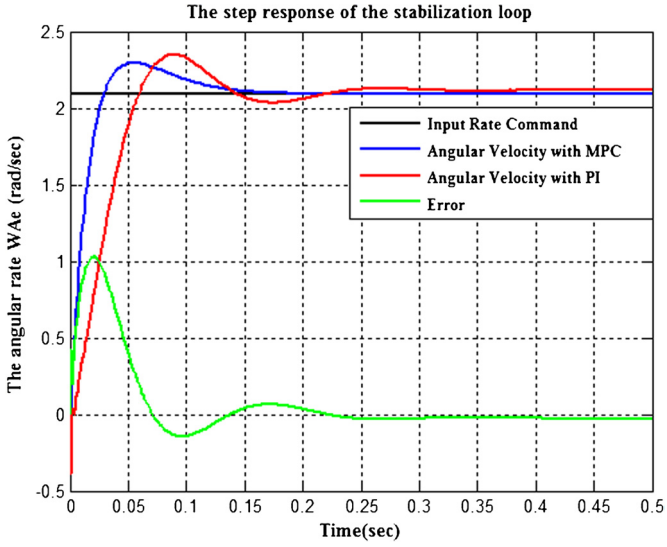

Fig. 7. Test number 2.

$$
\begin{aligned}
T_D &= (A_d - A_r)\omega_{Ar}\omega_{Ad}A_e\dot{\omega}_{Ae} \\
&= T_m + (A_d - A_r)\omega_{Ar}\omega_{Ad} + A_{rd}\left(\omega_{Ar}^2 - \omega_{Ad}^2\right) \\
&\quad - A_{de}(\dot{\omega}_{Ad} - \omega_{Ae}\omega_{Ar}) - A_{re}(\dot{\omega}_{Ar} + \omega_{Ae}\omega_{Ad}) \qquad (23)
\end{aligned}
$$

Fig. 6 shows the first test scenario by assuming the absence of disturbance torques (part A, test number 1). Also, Fig. 7 indicates the first test scenario by assuming the attendance of disturbance torques (part A, test number 2).

Fig. 8 and Fig. 9, the second test scenario assuming the absence of disturbance torques, in 2 seconds and 0.5 seconds respectively (part B, test number 3). Also, Fig. 10 and Fig. 11, the second test scenario assuming the presence of disturbance torques, in 2 seconds and 0.5 seconds respectively (part B, test number 4).

Fig. 12, shows the second test, for online input rate and angular rates, at flight path by imagining the presence of disturbance torques.

At the end, Figs. 13, 14 show the missile and target trajectory. Fig. 13 explains when the target is unformed of maneuver and Fig. 14 states when the target is composed of maneuver.

Based on the analysis of results indicated in Table 4, it can be noted that rising time, delaying times and settling time of PI con-

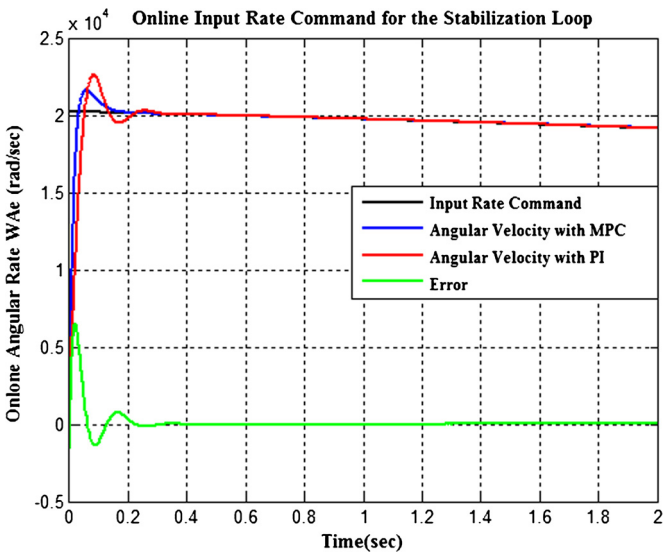

Fig. 8. Test number 3 in 2 s.

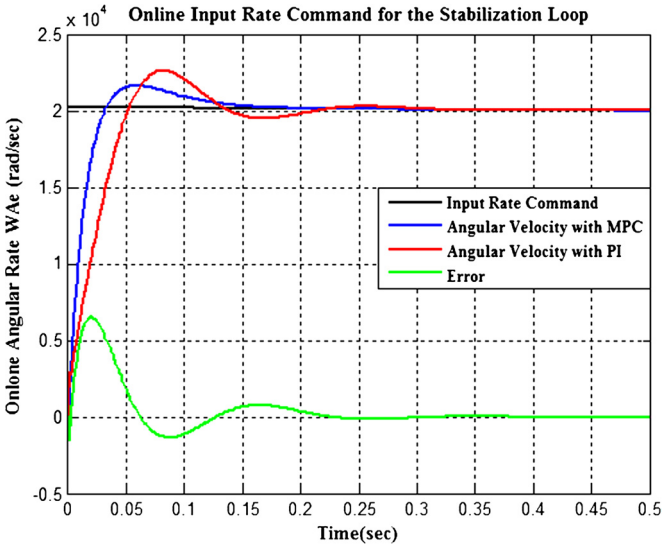

Fig. 9. Test number 3 in 0.5 s.

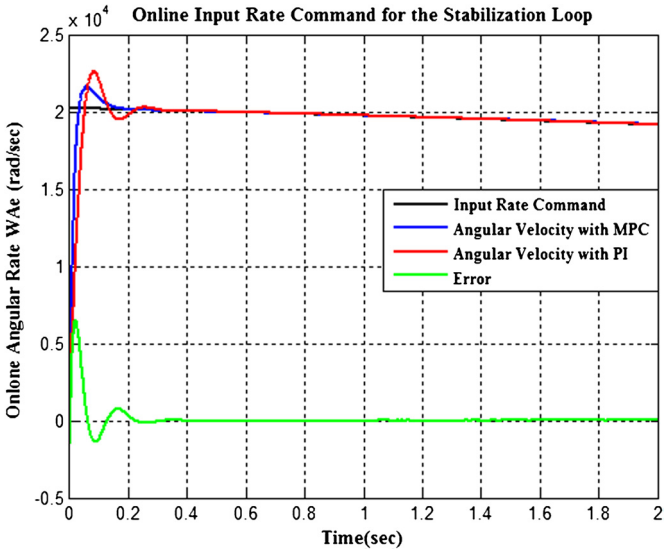

Fig. 10. Test number 4 in 2 s.

Table 4
Transient response analysis results.

Scenarios	Test number	PI controller				MPC controller			
		ov (%)	t_s (s)	t_d (s)	t_r (s)	ov (%)	t_s (s)	t_d (s)	t_r (s)
A	1	11.98	0.301	0.02011	0.0512	9.88	0.1999	0.008939	0.028
	2	12.17	0.35	0.02701	0.05823	9.59	0.1652	0.009077	0.02912
B	3	11.87	0.2946	0.02	0.05246	7.07	0.1742	0.01	0.03224
	4	11.91	0.3	0.01908	0.05288	6.7	0.1562	0.009	0.03316

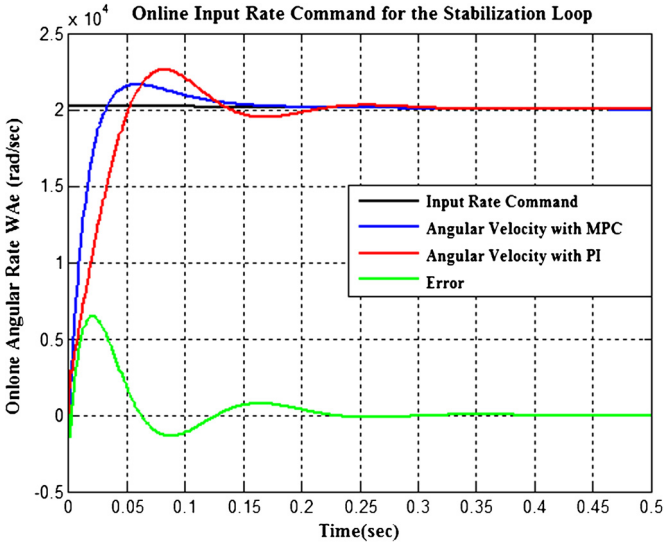

Fig. 11. Test number 4 in 0.5 s.

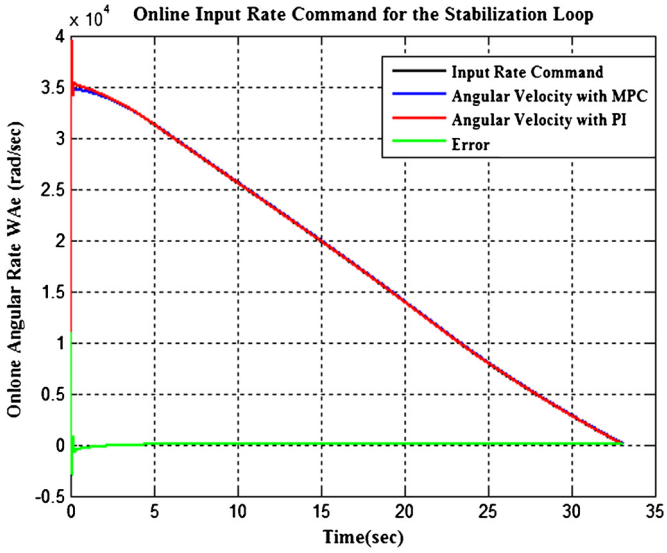

Fig. 12. Test at during the flight.

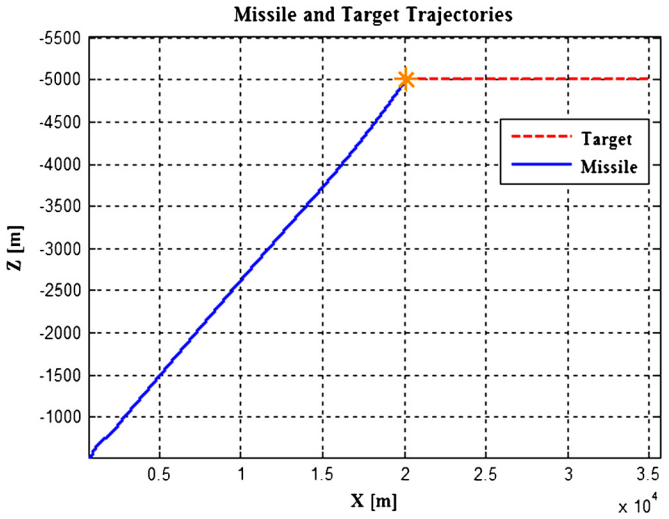

Fig. 13. Missile and target trajectories.

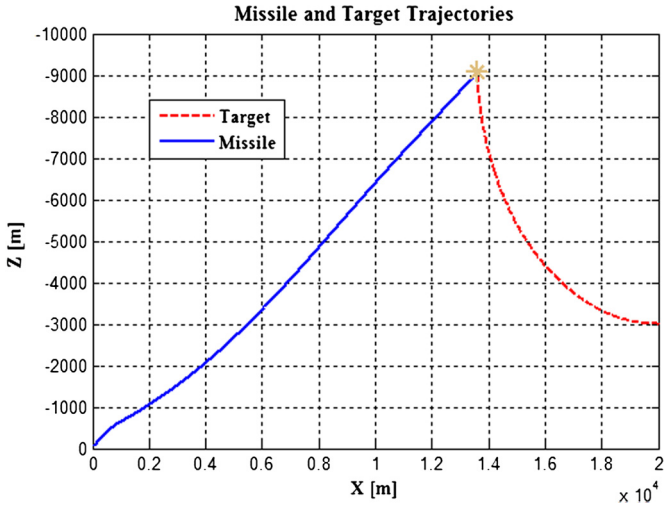

Fig. 14. Missile and target trajectories.

troller are more than those of MPC type controllers. Also, it can be mentioned that overshoot is reduced and the overall performance is highly improved in case of MPC type controller.

7. Conclusion

In this research, for evaluating the performance of gimbal system and one-axis gimbal system, we consider flight dynamics and test 6-DOF equations of motion. Accordingly, at first, we obtain the airframe dynamics and missile equations of motion. Then, we provide a model of one axis gimbal system with utilizing MPC type controller. Afterwards, guidance unit, autopilot and target specifications are modeled. Moreover, the system is modeled using SIMULINK/MATLAB. At the end, the system is tested for disturbance torques and angular velocities which are imposed online from missile frame to seeker. This paper successfully illustrates the application of the MPC controller to control one-axis gimbal system. Also, the response of the MPC is compared with that of traditional PI controller. The performances of the Stabilization loop with the MPC controller and PI controller have been tested in simulation. The obtained results prove that the MPC controller has very fast response, robustness in face of parameter uncertainty and disturbance torques, gimbal friction and mass unbalance. Also, the proposed MPC controller can reduce the response settling time in comparison with the PI controller. Thus, the proposed MPC controller develops the closeness of system response and supports the

system relative stability by reducing the response overshoot considerably.

Conflict of interest statement

None declared.

Appendix A. Supplementary material

Supplementary material related to this article can be found online at http://dx.doi.org/10.1016/j.ast.2016.04.019.

References

[1] M. Pirzadeh, A.R. Toloei, A.R. Vali, Effects of flight dynamics on performance of one axis gimbal system, considering disturbance torques, Int. J. Eng. (IJE), Trans. B: Appl. 28 (2015) 1108–1116.
[2] S.K. Chaudhuri, G. Venkatachalam, M. Prabhakar, Hardware-in-loop simulation for missile guidance and control systems, Def. Sci. J. 47 (1997) 343–357.
[3] Carlos E. García, David M. Prett, Manfred Morari, Model predictive control: theory and practice—a survey, Automatica 25 (1989) 335–348.
[4] D. Anderson, M. McGookin, Fast model predictive control of the Nadir singularity in electro-optic systems, J. Guid. Control Dyn. 32 (2009) 626–632.
[5] K. Salahshoor, A. Khaki-Sedigh, P. Sarhadi, An indirect adaptive predictive control for the pitch channel autopilot of a flight system, Aerosp. Sci. Technol. 45 (2015) 78–87.
[6] L. Wanli, Q. Xinghua, O. Jianfei, Modeling and simulation of laser tracking systems, Kybernetes 41 (2012) 1192–1199.
[7] M. Abdo, A.R. Toloei, A.R. Vali, M.R. Arvan, Modeling, control and simulation of cascade control servo system for one axis gimbal mechanism, Int. J. Eng. (IJE), Trans. A: Basics 27 (2013) 157–170.
[8] B. Kim, G.N. Washington, H.S. Yoon, Control and hysteresis reduction in prestressed curved unimorph actuators using model predictive control, J. Intell. Mater. Syst. Struct. 25 (2014) 290–307.
[9] T. Oktay, C. Sultan, Constrained predictive control of helicopters, Airc. Eng. Aerospace Technol. 85 (2013) 37–47.
[10] E. Joelianto, E.M. Sumarjono, A. Budiyono, D.R. Penggalih, Model predictive control for autonomous unmanned helicopters, Airc. Eng. Aerospace Technol. 83 (2011) 375–387.
[11] C.L. Lin, Y.H. Hsiao, Adaptive feedforward control for disturbance torque rejection in Seeker stabilizing loop, IEEE Trans. Control Syst. Technol. 9 (2001) 108–121.
[12] M. Abdo, A.R. Vali, A.R. Toloei, Fuzzy stabilization loop of one axis gimbal system, Int. J. Comput. Appl. 77 (2013) 6–13.
[13] S.T. Zhan, W.X. Yan, Z. Fu, G. Pan, Y.Z. Zhao, Robust control of a yaw-pitch gimbaled seeker, Airc. Eng. Aerospace Technol. 87 (2015) 83–91.
[14] Y.Sh. Kown, H.Y. Hwang, Y.S. Choi, Stabilization loop design on direct drive gimbaled platform with low stiffness and heavy inertia, in: Control, Automation and Systems, International Conference on ICCAS '07, 2007, 2007, pp. 320–325.
[15] Ch. Bai, Zh. Zhang, Acceleration-based mass imbalance feedforward compensation for inertial stabilized platform, J. Control Autom. Syst 12 (2014) 609–617.
[16] M. Abdo, A.R. Vali, A.R. Toloei, M.R. Arvan, Stabilization loop of a two axes gimbal system using self-tuning PID type fuzzy controller, ISA Trans. 53 (2014) 591–602.
[17] Sh. Yu, Y.Zh. Zhao, Study on rotational stabilization in a laser tracking system, J. Shanghai Jiaotong Univ. 14 (2009) 316–320.
[18] D.R. Otlowski, K. Wiener, B.A. Rathbun, Mass properties factors in achieving stable imagery from a gimbal mounted camera, in: SPIE, Airborne Intelligence, Surveillance, Reconnaissance (ISR) Systems and Applications V, vol. 6946, 2008.
[19] A. Khamis, A.M. Kamel, D.S. Naidu, Nonlinear optimal tracking for missile gimbaled seeker using finite-horizon state dependent Riccati equation, in: The 14th Annual IEEE International Conference on Cyber Technology in Automation, Control and Intelligent Systems, 2014, pp. 88–93.
[20] S. Mondal, S. Sadhu, A. Banerjee, Platform motion disturbances attenuation in a missile seeker subsystem using internal model control, in: International Conference on Control, Automation, Robotics and Embedded Systems (CARE), 2013, pp. 1–4.
[21] H. Zhuang, Z.S. Roth, Modeling gimbal axis misalignments and mirror center offset in a single-beam laser tracking measurement system, J. Robot. Res. 14 (1995) 211–224.
[22] A.K. Rue, Precision stabilization systems, aerospace and electronic systems, IEEE Trans. AES-10 (1974) 34–42.
[23] R.M. Gorecki, A Baseline 6 Degree of Freedom (DOF) Mathematical Model of a Generic Missile, DSTO Systems Science Laboratory, Australia, 2008.
[24] D.W. Clarke, C. Mohtadi, Properties of generalized predictive control, Automatica 25 (1989) 859–875.